Atmos. Meas. Tech. Discuss., https://doi.org/10.5194/amt-2018-45
Manuscript under review for journal Atmos. Meas. Tech.
Discussion started: 23 March 2018


Atmospheric Measurement Techniques Discussions

# Sensitivity of a Q-ACSM to chamber generated SOA with different oxidation states

Xiaoxiao Li[1], Yan Ma[2,3*], Hui Chen[2,3], Youling Jiang[2,3], Xin Ma[2,3], Rujin Yin[1], Dongsen Yang[2,3], Xiaowen Shi[2,3], Jiming Hao[1], Jingkun Jiang[1], and Jun Zheng[2,3*]

[1]State Key Joint Laboratory of Environment Simulation and Pollution Control, School of Environment, Tsinghua University, 100084 Beijing, China

[2]Collaborative Innovation Center of Atmospheric Environment and Equipment Technology, Nanjing University of Information Science & Technology, Nanjing 210044, China

[3]Joint Laboratory for Air Quality and Climate, Nanjing University of Information Science & Technology, Nanjing 210044, China

*Corresponding authors: Drs. Jun Zheng and Yan Ma*

*Email:* zheng.jun@nuist.edu.cn and mayan@nuist.edu.cn

*Address: School of Environmental Science and Engineering, Nanjing University of Information Science & Technology, Nanjing 210044, China*

*Tel.: +86-18251919852*

*Fax: +86-25-58731090*

**Abstract**

The accuracy in quantification of secondary organic aerosols (SOA) using a Q-ACSM has been comprehensively investigated in this work. SOA samples were generated under simulated photochemical oxidation conditions in a 4.5 $m^3$ Teflon chamber from three different volatile organic compounds (VOC) of atmospheric relevant concentrations (dozens of ppbv): α-pinene,

Atmos. Meas. Tech. Discuss., https://doi.org/10.5194/amt-2018-45
Manuscript under review for journal Atmos. Meas. Tech.
Discussion started: 23 March 2018


Atmospheric Measurement Techniques Discussions

isoprene, and toluene, representing both biogenic and anthropogenic VOC. Different SOA oxidation states were achieved by changing the relative ratio of the VOC precursor to the oxidants ($O_3$ or OH). A scanning mobility particle sizer (SMPS) and an aerosol particle mass analyzer (APM) were used to determine the number-size distribution and the exact mass of the chamber-generated SOA, which were then used to deduce the SOA effective density and mass concentration. Results showed that aerosol mass concentration measured by the Q-ACSM based on SMPS calibration alone may be associated with considerable errors due to the fact that the effective density of SOA at different oxidation state can change substantially. More importantly, the sensitivity of the Q-ACSM to a specific type of SOA was found to be anti-correlated with the aerosol oxidation state regardless of the VOC precursors. This may be due to the decreasing of relative ionization efficiency (RIE) or the collection efficiency (CE) of the Q-ACSM for more oxidized SOA. To pinpoint the actual cause, ammonium sulfate ($(NH_4)_2SO_4$) seed particles were injected into the chamber before SOAs were produced and the CE for a specific SOA sample was hence determined with reference to the changes in sulfate signals. Our experiment results along with previous literature reports strongly implied that as the SOA oxidation state increases, SOA will transform gradually from a liquid state (CE ≈ 1) into a solid (or glassy) state with a CE of 0.2~0.5. Meanwhile, the RIE of OA decreased substantially when SOA transformed from hydrocarbon-like OA (HOA) into more oxygenated OA (OOA) and may further decrease as O/C continued to increase. Our results indicated that the current Q-ACSM calibration procedure using a constant RIE may lead to somewhat underestimation of more oxidized OOA but overestimation of less oxidized HOA, i.e., a variable RIE shall be applied, most likely as a function of the SOA oxidation state.

**Key words:** Organic Aerosol; ACSM Calibration; Relative Ionization Efficiency; Collection Efficiency; Effective Density.

Atmos. Meas. Tech. Discuss., https://doi.org/10.5194/amt-2018-45
Manuscript under review for journal Atmos. Meas. Tech.
Discussion started: 23 March 2018




## 1. Introduction

Organic aerosol (OA) have been recognized as a major component in ambient particles, contributing 20-90% to the total submicron particles around the world (Hallquist et al., 2009a; Kanakidou et al., 2005; Salcedo et al., 2006; Zhang et al., 2007), which can substantially affect the climate directly by interacting with solar radiation and indirectly by affecting cloud microphysics (IPCC, 2014). Recent studies demonstrated that haze events in China were largely driven by secondary organic aerosol (SOA) (Huang et al., 2014) and may exert significant adverse effects on human health (Poschl, 2005; Poschl and Shiraiwa, 2015). The chemical composition and the dramatic changes of OA in ambient remain less understood compared to the inorganic species. Measurements of OA has been a challenging task not only for the fact that OA contains nearly countless chemical species but also due to its relatively short lifetime and rapid transformation in the atmosphere. Traditionally, the sampling and the ensuing chemical analyses of aerosol composition are mainly utilizing filter based offline methods, followed by analysis with gas chromatography/mass spectrometry (GC/MS), liquid chromatograph/mass spectrometry (LC/MS), nuclear magnetic resonance(NMR) or Fourier transform infrared spectroscopy (FTIR). Evidently, offline techniques cannot catch the dramatic change of ambient OA (Hallquist et al., 2009b). Therefore, many in-situ instrumentations have been developed to conduct aerosol measurements in real time. For example, the particles-into-liquid sampler system (PILS) (Sorooshian et al., 2006) firstly strips out the gas-phase pollutants and dissolves remaining particulate samples into water solutions, which are then send to ion chromatography for further analyses. Clearly, PILS can prevent sample loss by eliminating pre-processing processes. However, only water-soluble components can be analyzed by PILS and no size-resolved measurement can be achieved (Orsini et al., 2003; Weber et al., 2001). Similarly, another widely used thermal-optical organic carbon/elementary carbon (OC/EC) analyzers can only quantify total OC with very limited information (Birch and Cary, 1996).

Atmos. Meas. Tech. Discuss., https://doi.org/10.5194/amt-2018-45
Manuscript under review for journal Atmos. Meas. Tech.
Discussion started: 23 March 2018


Atmospheric Measurement Techniques Discussions

Recently, a new powerful method, known as aerosol mass spectrometry (AMS) has been successfully developed and widely deployed to do size-resolved aerosol measurements in real time (Jayne et al., 2000). A typical AMS is equipped with a set of aerodynamic lens (Liu et al., 1995a, b) to effectively focus and transmit particles (~50 - 1000 nm) ($PM_1$) into the instrument, a time-of-flight (ToF) chamber to determine the aerosol size, a thermal vaporizer (heated to ~600°C) to evaporate non-refractory (NR) components into the gas-phase, and a 70 eV electron impact (EI) ionization source to ionize the gaseous samples before they can be analyzed by a mass analyzer (either a quadrupole or a time-of-flight mass spectrometer) (DeCarlo et al., 2004; Jayne et al., 2000). Evidently, compared to previous techniques, AMS can provide elemental composition of the organic species and can achieve much higher time and size resolution. More recently, a newer version of AMS, i.e., the aerosol chemical speciation monitor (ACSM) was developed (Ng et al., 2011). ACSM is basically a simplified AMS without the aerosol ToF chamber and thus is much smaller and affordable. Although ACSM cannot obtain high resolution mass spectra, elementary information can still be readily recovered from some symbolic fragments, such as $C_nH_{2n+1}$ (*m/z* 27, 29, 41, 43, 55, 57, 69…) and $CO_2^+$ (*m/z* 44), representing hydrocarbon-like organic aerosol (HOA) and oxygenated organic aerosol (OOA) (Ng et al., 2011). Therefore, ACSM is especially suitable for long term field operation. Nevertheless, Aerodyne AMS/ACSM have been widely used to conduct researches on NR-$PM_1$ around the world in both field and chamber studies (Zhang et al., 2007; Zhou et al., 2016).

Although the performance of AMS/ACSM has been demonstrated to be in accordance with many other measuring techniques (Drewnick et al., 2003; Jimenez et al., 2016; Kondo et al., 2007; Takegawa et al., 2005), the quantification of aerosol composition by AMS/ACSM still needs to be further refined. In theory, the sensitivity of AMS is affected by the particle transmission efficiency through the aerodynamic lens, the ion transmission efficiency inside the mass analyzer, the particle collection efficiency (CE) by the vaporizer due to the bouncing effect, the ionization efficiency (IE)

Atmos. Meas. Tech. Discuss., https://doi.org/10.5194/amt-2018-45
Manuscript under review for journal Atmos. Meas. Tech.
Discussion started: 23 March 2018




and the possible fragmentation during the thermo-vaporization and EI ionization (70eV) (Allan et al., 2003; Canagaratna et al., 2015; Jayne et al., 2000; Jimenez et al., 2003). In practice, AMS calibrations in terms of CE and IE are mostly conducted with inorganic species only and the calibration factors for organics are indirectly inferred and can be highly uncertain (Jimenez et al., 2016).

It has been suggested that CE can be affected by particle chemical composition, particle phase, particle size as well as RH. Based on inter-comparisons in sulfate measurements between AMS, PILS-IC and other instruments, a CE of 0.5 for all compounds has been recommended with the assumption that particles are internally mixed (Drewnick et al., 2003; Takegawa et al., 2005). Although organics quantified using a CE of 0.5 has been found correlating well with independent OC or VOCs measurement in most field works (Allan et al., 2004; de Gouw et al., 2005; Takegawa et al., 2005; Venkatachari et al., 2006), studies have shown that CE can vary substantially for various chamber generated organic particles (Bahreini et al., 2005; Docherty et al., 2013). Similarly, IE of inorganic components is usually calibrated directly with ammonium sulfate ($(NH_4)_2SO_4$) and ammonium nitrate ($NH_4NO_3$) aerosols of known mass concentration, while the organic components is assigned with a constant relative ionization efficiency (RIE, i.e., the ratio of the electron impact ionization efficiency of a given species to the measured ionization efficiency of nitrate on a per unit mass basis) of 1.4. However, RIE of organic aerosols ($RIE_{org}$) has been suggested to be significantly different for different OA species (Murphy, 2016). For instance, it appears that the RIE values of primary OA (POA) are significantly different from those of SOA (Dzepina et al., 2007; Jimenez et al., 2016; Slowik et al., 2004). Any uncertainty associated with the $RIE_{org}$ may lead to erroneous AMS/ACSM measurement results, especially in the case of interpreting aerosol samples from various environment around the world. Therefore, comprehensive researches on the CE and RIE of different SOA species are of practical importance to constrain the AMS/ACSM measurements. Some methods have been introduced to quantify or



eliminate the side-effects of RIE and CE in AMS measurements. For example, using laser-based vaporizer makes it possible to directly measure aerosol CE (Cross et al., 2007). However, the laser can only be used for particles larger than 250 nm. Most recently, a new type of capture vaporizer has been developed to achieve a unit CE (Hu et al., 2017). However, the capture vaporizer will increase the residence time of aerosol inside the vaporizer and thus change the fragmentation pattern to produce many smaller fragments, which will highly complicate the AMS quantification process.

In this work, the performance of a quadrupole based ACSM (Q-ACSM) was comprehensively investigated for chamber-generated SOA samples under simulated photochemical oxidation conditions, including both hydroxyl radical (OH) oxidations and ozonolysis ($O_3$). Three different volatile organic compounds (VOC) (i.e., α-pinene, isoprene, and toluene) at atmospheric relevant concentrations (dozens of ppbv) were chosen to represent both biogenic and anthropogenic VOC. The SOA mass concentrations were directly measured by an aerosol particle mass analyzer (APM) to achieve higher accuracy. The sensitivity of Q-ACSM to SOA at different oxidation state or O/C ratio was quantified.

## 2. Experimental Methods

### *2.1 Chamber Setup*

A 4.5 $m^3$ collapsible atmospheric-pressure fluoropolymer (Teflon) smog chamber (L = 1.8 m; W = 1.5 m; H = 1.7 m) (see Fig. 1) was used to generate organic aerosols under atmospheric relevant conditions. The chamber was essentially the same as the one used in our earlier work (Yao et al., 2014; Yuan et al., 2017) and has been described in details previously. Before each set of the experiments, the chamber was thoroughly cleaned by irradiation with black light UV-lamps and exposure to a high concentration (a few ppmv) of $O_3$ for more than 6 hours. Before each experiment, the chamber was flushed by pure air generated by a zero-air generator (Acdco 737) until less than



10 particles $cm^{-3}$ was detected inside the chamber. Reactants and scavengers (if used) were carried into the chamber through a T-shaped glass bulb by pure air. The glass ball was heated gently to insure completely injection. At the bottom center of the smog chamber was installed a Teflon coated fan for rapid mixing of all reactants. The chamber temperature and RH were maintained at 20±1°C and 10%-15%, respectively.

### *2.2 SOA Generation*

During each experiment, known amount of α-pinene (Sigma-Aldrich, >98%), isoprene (Sigma-Aldrich, >99%), or toluene (Sigma-Aldrich, >99.5%) was firstly dissolved into cyclohexane (TEDIA Inc., HPLC grade >99.5%) and then was injected into the chamber through a stream of pure air. The concentrations of these precursor VOCs were set to atmospheric relevant levels to make the results of this work more applicable to ambient measurements. Ozone was generated by exposing pure oxygen ($O_2$) to a low-pressure mercury (Hg) lamp (Jelight, Model 600). When $O_3$ was used as the oxidant, OH radical scavenger, cyclohexane, was injected into the chamber before the experiment. When OH was used as the oxidant, trace amount of self-synthesized methyl nitrite was firstly injected into the chamber and then the black light bulbs around the chamber were turned on for several minutes to start the OH-initiated oxidations (Yao et al., 2014). The mixing ratios of $O_3$ inside the chamber was monitored continuously by a Thermo Fisher Scientific ozone monitor (Model 49i) throughout the experiment. Different SOA oxidation states were achieved by changing the ratio between the VOC precursor and the oxidant ($O_3$ or OH).

### *2.3 Q-ACSM Operation*

The sampling interval of Q-ACSM was set to be 8-15 minutes, depending on the particle mass concentration generated in the chamber. The sampling tube was made of a 6.3 mm OD, 0.8 m long stainless-steel tube. One liter per minute (lpm) air was sampled from the chamber instead of the original 3 lpm to minimize the total gases pulled out from the chamber. The Ionization efficiency

Atmos. Meas. Tech. Discuss., https://doi.org/10.5194/amt-2018-45
Manuscript under review for journal Atmos. Meas. Tech.
Discussion started: 23 March 2018


Atmospheric Measurement Techniques Discussions

for $NO_3^-$ of Q-ACSM was calibrated before and after each experiment using $NH_4NO_3$ following the procedure described by Ng et al. (2011). The measured organic mass concentration was calculated using a default RIE value of 1.4 and a CE value of 0.5, which have been widely used during most of the field and laboratory measurements (Canagaratna et al., 2007). The nitrogen ($N_2$) peak ($m/z$ = 28) and the internal naphthalene standard peak ($m/z$ = 128) were used before the experiment to do mass calibration. The mass dependent transmission efficiency of the Q-mass spectrometer was also calibrated before data analyses.

### *2.4 Aerosol Mass Measurement*

A scanning mobility particle sizer (SMPS), consisting of a differential mobility analyzer (DMA, TSI Model 3081) and a condensation particle counter (CPC, TSI Model 3776), was used for real-time monitoring of the particle number size distribution between 15 nm-650 nm particles and aerosol volume concentrations were deduced assuming spherical shape. The time resolution was 5 mins. An aerosol particle mass analyzer (APM, Kanomax Model 3601) combined with a DMA (TSI Model 3081) and a CPC (TSI Model 3776) were used to determine the particle mass and thus the particle effective density (ρ) was calculated from the measured mobility diameter (DeCarlo et al., 2004; McMurry et al., 2002). During each experiment, the diameter of the particle to be analyzed by the APM was manually set to be the same as the peak value of the particle number size distribution measured by the SMPS, as the particles were continuously growing in the chamber. One DMA-APM scan took about 5 mins. Hence, the particle mass concentration was calculated from the measured particle volume concentration and the corresponding effective density.

## 3. Results and Discussion

### *3.1 Determine the Q-ACSM Response Factor for Chamber Generated SOA*

The evolution of SOA during a typical chamber experiment was shown in Fig. 2, where 80 ppbv $O_3$ and 20 ppbv α-pinene were injected into the chamber. Shortly after injection, strong



196 nucleation event occurred and was marked by a typical banana-shaped three-dimensional (3-D)
197 number size distribution plot (Fig. 2a). Figure 2b showed the time series of aerosol mass
198 concentrations measured by Q-ACSM, integrated from SMPS measurements, and the
199 corresponding f44 (the ratio of *m/z* 44 signal over total organic ion signal intensity) and effective
200 density of aerosol calculated from the Q-ACSM and APM measurements, respectively. Since *m/z*
201 44 signal basically reflected the oxygen content in OA, the O/C ratio can be deduced directly from
202 f44, both of which have been widely used to represent the oxidation state of OA (Canagaratna et
203 al., 2015). The number size-distributions at one hour interval during the chamber experiment were
204 also depicted in Fig. 2c. Evidently, as the ozonolysis reaction proceeded, the size and mass
205 concentration of the aerosol swiftly increased, especially during the initial two hours. The effective
206 density of the formed aerosol also increased as the aerosol became more compact and approached
207 a spherical shape. The initial high values of f44 may be due to the fact that initially formed SOA
208 particles were highly oxidized because of gas/particle partitioning (Shilling et al., 2009a) . The f44
209 factor in the following period fluctuated between 0.115 and 0.135, indicating that the oxidation
210 state of aerosols did not change significantly within the experimental period. After 2~3 hours, the
211 aerosol size reached 80~100 nm, mass concentration increased to 40~50 μg $m^{-3}$, and the effective
212 density and f44 were about 1.2 g $cm^{-3}$ and 0.13, respectively. By then a relative steady-state was
213 reached and the response factor (RF) of the Q-ACSM was thus determined through a linear
214 correlation analysis using the relative steady-state data, as shown in Fig. 3.

215 In a similarly way, fourteen independent chamber experiments were conducted in this work.
216 Each experiment typically lasted for 4-6 hours until f44, effective density, and mass concentration
217 all reached relatively steady states. The slight variation of f44 after reaching relatively steady state
218 in each experiment was mainly due to the measurement uncertainty associated with the Q-ACSM.
219 The VOC used in this work included α-pinene, isoprene, and toluene, representing both biogenic
220 and anthropogenic VOC emissions. Both ozonolysis and OH initiated oxidation processes were

Atmos. Meas. Tech. Discuss., https://doi.org/10.5194/amt-2018-45
Manuscript under review for journal Atmos. Meas. Tech.
Discussion started: 23 March 2018




studied except that in the case of toluene only OH reactions were investigated. To generate SOA samples under atmospheric relevant conditions and thus avoid secondary VOC oxidation products, the mixing ratios of these VOC precursors ranged from 10 to 60 ppbv for α-pinene, 60 to 200 ppbv for isoprene, and 30 to 60 ppbv for toluene. The oxidant concentrations were also limited to 50-80 ppbv for $O_3$ and 50-300 μL for methyl nitrite. The detailed experimental conditions and results were listed in Table 1.

### *3.2 Effects of f44*

To investigate the effects of oxidation state of the SOA samples (i.e., the measured f44) on the Q-ACSM detection sensitivity, for each pair of VOC/oxidant several experiments were repeated with different relative concentration ratio between the VOC and the oxidant. Evidently, the characteristics of the generated SOA from the oxidation of isoprene, α-pinene, and toluene appeared to be significantly different among various oxidation conditions. Especially the RF of the Q-ACSM changed substantially for different f44. Both isoprene and α-pinene are relatively reactive toward $O_3$ and OH. However, the dominant degradation processes in the atmosphere for isoprene and α-pinene are typically through oxidations by OH and $O_3$, respectively. Especially, laboratory studies have shown that the ozonolysis of α-pinene can lead to considerably higher SOA yield than that from OH initiated reactions (Yao et al., 2014). Therefore, in this work we were focusing on the isoprene-OH and α-pinene-$O_3$ reactions only. In the case of toluene, the experiment was relatively straightforward since toluene only reacted with OH radicals. The oxidation states of SOA generated in each experiment was shown in different colors in triangle plot (see Fig. 4). Since some $O_3$ will be produced during OH initiated chain reactions (Finlayson-Pitts and Pitts, 1999), the oxidation state of isoprene-generated SOA varied more significantly as the experiment proceed. For α-pinene, however, f44 did not vary considerably as isoprene during the one experiment period and in between experiments. Even when $O_3$ to α-pinene ratio was increased substantially, only slight increase in f44 was observed, which was most likely due to the fact that the first-generation

Atmos. Meas. Tech. Discuss., https://doi.org/10.5194/amt-2018-45
Manuscript under review for journal Atmos. Meas. Tech.
Discussion started: 23 March 2018


Atmospheric Measurement Techniques Discussions

246 oxidation products of α-pinene were mainly partitioned into the aerosol phase and cannot be further
247 oxidized by $O_3$. Nevertheless, the Q-ACSM RF for all chamber-generated SOA decreased linearly
248 as the f44 increased (see Fig. 5a).

249 The effective density of all chamber-generated SOA ranged between 1.09-1.36 g $cm^{-3}$, which
250 covered a much larger range compared to the reported values of 1.22-1.28 by Zelenyuk et al. (2008)
251 and 1.3±0.1 by Kiendler-Scharr et al. (2009) for biogenic SOA. Also, clearly shown in Fig. 5b was
252 that the SOA effective density increased linearly with increasing f44, most likely due to the fact
253 that when more oxidants were present, more highly oxygenated products were produced and led to
254 the formation of more compact SOA. Our results indicated that the oxidation state and effective
255 density of atmospheric SOA may vary significantly from different ambient oxidation environment
256 and can change dynamically at different stage of the aging process. Therefore, it was reasonable to
257 assume that quantification of ambient OA by Q-ACSM using a constant conversion factor may
258 induce significant error in aerosol mass concentration. Accordingly, the Q-ACSM RF for OA
259 should be systematically calibrated with laboratory-generated aerosols produced not only from
260 various VOC precursors but also under different atmospheric-relevant reaction conditions.

261 Typically, Q-ACSM RF for OA is determined indirectly using nitrate salt standards as
262 reference and can be mathematically expressed as the product of three factors:

263 $$RF = IE_{NO3} \cdot RIE_{org} \cdot CE_{org}, \quad (E1)$$

264 i.e., the ionization efficiency of nitrate salt ($IE_{NO3}$), the relative ionization efficiency of OA ($RIE_{org}$),
265 and the collection efficiency of OA ($CE_{org}$) of the Q-ACSM. $IE_{NO3}$ can be calibrated before and
266 after the experiments and is independent from the properties of OA. However, the other two terms
267 may vary with different OA samples, the observed anti-correlation of RF with f44 could be due to
268 either CE or RIE.

269 ***3.3 Effects of CE***

Atmos. Meas. Tech. Discuss., https://doi.org/10.5194/amt-2018-45
Manuscript under review for journal Atmos. Meas. Tech.
Discussion started: 23 March 2018




To investigate and evaluate the possibility that CE may contribute to the observed anti-correlations between RF and f44 in this work, a set of chamber experiments using $(NH_4)_2SO_4$ (AS) seed particles were conducted. The difference between this set of experiments from the previous ones was that here nebulized dry AS seed particles were injected into the chamber before the SOA was produced, i.e., the gas phase products will condense onto the AS seed surface instead of initiating new particle formation. After fully coated with SOA, the measured sulfate mass concentration by Q-ACSM will change due to variation in $CE_{SO4}$ and the CE of SOA material ($CE_{org}$) can be deduced accordingly. In each experiment, similar amount and size of AS seeds were used to avoid other possible affecting factors. Figure 6 displayed the time series of a typical AS chamber experiment. Initially, AS seed aerosol was injected and ACSM measured sulfate mass concentration was about 35 μg $m^{-3}$. After VOC precursor was injected, the ACSM measured sulfate increased rapidly to about 50 μg $m^{-3}$. As shown in Fig. 6, the sulfate signal increased substantially after coated with SOA but the measured f44 did not change significantly as SOA was continuously produced. Thus, $CE_{org}$ at certain f44 can be evaluated. Evidently, the accuracy of the absolute value of $CE_{org}$ will depend on $CE_{SO4}$ and $RIE_{SO4}$. It is worth noting that $CE_{SO4}$ may vary from 0.2 to 1 as a function of RH (Matthew et al., 2008). $CE_{SO4}$ was measured to be 0.28 in this work with RH<15%. In the case of $RIE_{SO4}$, a value of 1.15 was used here as suggested by other studies (Canagaratna et al., 2007; Ng et al., 2011; Petit et al., 2015). Although recent researches have shown that $RIE_{SO4}$ may vary from instrument to instrument (Budisulistiorini et al., 2014; Crenn et al., 2015), the exact $RIE_{SO4}$ value would not affect the conclusion of this research. For the scope of this work, only the relative changes in sulfate concentration were noted.

Total nine AS-chamber experiments were conducted in this work and the detailed experiment conditions and results were listed in Table 2. However, $CE_{org}$ appeared to be affected by the SOA coating thickness (see Fig. 7), which would decide the mixing state of the SOA coated AS particles. When the coating material was not enough to fully cover the seed particles (dark blue points), there


295 was a possibility that the seed core would hit the collection surface directly and thus behaved as an
296 AS particle. To demonstrate this possibility, an experiment under extreme condition was conducted,
297 i.e., substantially excess VOC precursor was added. The result was indicated by the red point in
298 Fig. 7. This near unit CE (~0.97) suggested that the AS aerosols were fully covered with SOA and
299 behaved as a pure SOA, which may assume a "sticky" liquid state. However, no higher f44 values
300 could be achieved with such large amount of organics generated, which was possibly related to the
301 loading-dependent gas-particle partitioning (Shilling et al., 2009b) and made it difficult to address
302 f44 influence on $CE_{org}$ via experiment. The coating layer of the light blue points should be thick
303 enough to cover the AS core, which was indicated by the decreasing $CE_{org}$ from 1 to ~0.5 with
304 increasing f44. However, there was still a possibility that the CE values of these light blue points
305 were the results of a combination of AS core and organic shell.

306 CE for biogenic SOA has been reported to be close to one based on both chamber experiments
307 (Kiendler-Scharr et al., 2009) and field measurements conducted in amazon, where aerosols were
308 dominated by liquid SOA (Allan et al., 2014; Chen et al., 2009). However recently, it has been
309 proposed in theoretical, chamber, and field studies that organic particles can exist in semi-solid or
310 solid state under ambient temperature, rather than been in liquid state (Shiraiwa et al., 2011; Vaden
311 et al., 2010; Virtanen et al., 2010).

312 The oxidation products of VOCs under ambient conditions are mainly consisted of carbonyl
313 compounds and carboxylic acids (Finlayson-Pitts and Pitts, 1999), the saturation vapor pressures
314 of which normally decrease with increasing oxidation level. As they are more oxidized, SOA may
315 transit from liquid phase gradually into solid phase under ambient temperature, which are consistent
316 with our observations of higher effective density at higher oxidation state. Accordingly, the surface
317 property of SOA can change dramatically and may induce considerable change in CE as SOA
318 transforms from a "sticky" liquid-drop into a "bouncing" solid-ball. Particle morphology research
319 based on glass transition temperature ($T_g$) indicated that during oxidation, the SOA particles will

Atmos. Meas. Tech. Discuss., https://doi.org/10.5194/amt-2018-45
Manuscript under review for journal Atmos. Meas. Tech.
Discussion started: 23 March 2018


Atmospheric Measurement Techniques Discussions

change from liquid state to semi-solid state and finally to solid or glassy state (Koop et al., 2011), resulting from a combined effect of increasing molecular weight and O/C. In previous studies, $CE_{org}$ has also been demonstrated to be variable for particles of different chemical composition, phase and under different RH, with a value ranging from 0.2 to ~1 (Alfarra, 2004; Docherty et al., 2013).

### *3.4 Effects of RIE*

RIE for a specific molecule can be evaluated as following (Canagaratna et al., 2007; Jimenez et al., 2003):

$$\mathrm{RIEs} = \frac{\mathrm{MW_{NO3}}}{\mathrm{IE_{NO3}}} \cdot \frac{\mathrm{IEs}}{\mathrm{MWs}}, \qquad \text{(E2)}$$

where RIEs is the relative ionization efficiency for a specific organic molecule S. IEs and MWs are respectively the ionization efficiency and the molecular weight of S. Theoretically, IEs is directly proportion to σ, i.e., the electron impact ionization cross section of the molecule, which is linearly related to the number of electrons in the molecule. Since the number of electrons is roughly proportional to the molecular weight, RIEs of molecules with similar structure and function groups are suggested to be similar to each other. RIEs values for hydrocarbons and oxygenated species, however, are believed to be different since their oxygen contents can vary substantially (Canagaratna et al., 2007), ranging from less than 1 to more than 3 (Dzepina et al., 2007; Jimenez et al., 2016; Slowik et al., 2004). Consequently, the anti-correlation between RF and f44 may also due to different RIEs related to the oxygen contents.

## 4. Conclusion

The sensitivity of Q-ACSM to chamber-generated SOA in various oxidation states was comprehensively investigated and an anti-correlation between the instrument sensitivity, RF, and SOA oxidation state, represented by f44, was obtained regardless of the type of VOC precursors. Therefore, our results strongly indicated that ambient OA measurements by Q-ACSM using a



343 constant conversion factor may induce significant error in aerosol mass concentration. Accordingly,
344 the Q-ACSM RF for OA should be systematically calibrated with laboratory-generated aerosols
345 produced not only from various VOC precursors but also under different atmospheric-relevant
346 reaction conditions. Based on our chamber experiment results and previously reported observation
347 in chamber and ambient studies, a comprehensive view of $RF_{org}$, $RIE_{org}$, $CE_{org}$, and $\rho_{effective}$ of OA
348 at different oxidation state (indicated by f44) was proposed (see Fig. 8). It was reasonably to assume
349 that as a SOA particle was in low oxidation state, it was basically in liquid state with a CE of close
350 to one. With the increase of O/C, the liquid state slowly changed into semi-solid and finally the
351 solid/glassy state with a CE ranging from 0.2~0.5. The RIE of organics would decrease
352 substantially from hydrocarbon-like compounds to oxygen containing compounds but would only
353 continue to decrease at a slower rate with further increasing O/C. The observed anti-correlation
354 between RF and O/C in this work can be explained by the combined effects of CE and RIE. Our
355 results suggested that under certain circumstance a Q-ACSM calibrated using the traditional
356 method may underestimate OOA content but overestimate HOA in previous studies. Accordingly,
357 different $RIE_{org}$ values should be used for HOA and OOA. In addition, early AMS calibrations
358 based on SMPS measured mass concentration may be associated with considerable errors due to
359 the fact that the effective density of SOA at different oxidation state can change substantially.

360 ***Acknowledgements***

361 This work is supported by the National Key Research and Development Project
362 (2016YFC0202401), National Natural Science Foundation of China (41575122, 41675126, and
363 41730106), and the Priority Academic Program Development of Jiangsu Higher Education
364 Institutions. The data used are listed in the tables and references. The data used in this work are
365 available from the authors upon request (zheng.jun@nuist.edu.cn).

366



## References

Alfarra, M.: Insights into atmospheric organic aerosols using an aerosol mass spectrometer, University of Manchester, 2004.

Allan, J. D., Alfarra, M. R., Bower, K. N., Williams, P. I., Gallagher, M. W., Jimenez, J. L., McDonald, A. G., Nemitz, E., Canagaratna, M. R., Jayne, J. T., Coe, H., and Worsnop, D. R.: Quantitative sampling using an Aerodyne aerosol mass spectrometer: 2. Measurements of fine particulate chemical composition in two UK cities, J. Geophys. Res.-Atmos., 108, 10.1029/2003jd001608, 2003.

Allan, J. D., Bower, K. N., Coe, H., Boudries, H., Jayne, J. T., Canagaratna, M. R., Millet, D. B., Goldstein, A. H., Quinn, P. K., Weber, R. J., and Worsnop, D. R.: Submicron aerosol composition at Trinidad Head, California, during ITCT 2K2: Its relationship with gas phase volatile organic carbon and assessment of instrument performance, J. Geophys. Res.-Atmos., 109, 10.1029/2003jd004208, 2004.

Allan, J. D., Morgan, W. T., Darbyshire, E., Flynn, M. J., Williams, P. I., Oram, D. E., Artaxo, P., Brito, J., Lee, J. D., and Coe, H.: Airborne observations of IEPOX-derived isoprene SOA in the Amazon during SAMBBA, Atmos Chem Phys, 14, 11393-11407, 10.5194/acp-14-11393-2014, 2014.

Bahreini, R., Keywood, M. D., Ng, N. L., Varutbangkul, V., Gao, S., Flagan, R. C., Seinfeld, J. H., Worsnop, D. R., and Jimenez, J. L.: Measurements of secondary organic aerosol from oxidation of cycloalkenes, terpenes, and m-xylene using an Aerodyne aerosol mass spectrometer, Environ. Sci. Technol., 39, 5674-5688, 10.1021/es048061a, 2005.

Birch, M. E., and Cary, R. A.: Elemental carbon-based method for monitoring occupational exposures to particulate diesel exhaust, Aerosol Sci. Technol., 25, 221-241, 10.1080/02786829608965393, 1996.

Budisulistiorini, S. H., Canagaratna, M. R., Croteau, P. L., Baumann, K., Edgerton, E. S., Kollman, M. S., Ng, N. L., Verma, V., Shaw, S. L., Knipping, E. M., Worsnop, D. R., Jayne, J. T., Weber, R. J., and Surratt, J. D.: Intercomparison of an Aerosol Chemical Speciation Monitor (ACSM) with ambient fine aerosol measurements in downtown Atlanta, Georgia, Atmos. Meas. Tech., 7, 1929-1941, 10.5194/amt-7-1929-2014, 2014.

Canagaratna, M. R., Jayne, J. T., Jimenez, J. L., Allan, J. D., Alfarra, M. R., Zhang, Q., Onasch, T. B., Drewnick, F., Coe, H., Middlebrook, A., Delia, A., Williams, L. R., Trimborn, A. M., Northway, M. J., DeCarlo, P. F., Kolb, C. E., Davidovits, P., and Worsnop, D. R.: Chemical and microphysical characterization of ambient aerosols with the aerodyne aerosol mass spectrometer, Mass Spectrom. Rev., 26, 185-222, 10.1002/mas.20115, 2007.



Canagaratna, M. R., Jimenez, J. L., Kroll, J. H., Chen, Q., Kessler, S. H., Massoli, P., Hildebrandt Ruiz, L., Fortner, E., Williams, L. R., Wilson, K. R., Surratt, J. D., Donahue, N. M., Jayne, J. T., and Worsnop, D. R.: Elemental ratio measurements of organic compounds using aerosol mass spectrometry: characterization, improved calibration, and implications, Atmos. Chem. Phys., 15, 253-272, 10.5194/acp-15-253-2015, 2015.

Chen, Q., Farmer, D. K., Schneider, J., Zorn, S. R., Heald, C. L., Karl, T. G., Guenther, A., Allan, J. D., Robinson, N., Coe, H., Kimmel, J. R., Pauliquevis, T., Borrmann, S., Poeschl, U., Andreae, M. O., Artaxo, P., Jimenez, J. L., and Martin, S. T.: Mass spectral characterization of submicron biogenic organic particles in the Amazon Basin, Geophys. Res. Letts., 36, 10.1029/2009gl039880, 2009.

Crenn, V., Sciare, J., Croteau, P. L., Verlhac, S., Froehlich, R., Belis, C. A., Aas, W., Aijala, M., Alastuey, A., Artinano, B., Baisnee, D., Bonnaire, N., Bressi, M., Canagaratna, M., Canonaco, F., Carbone, C., Cavalli, F., Coz, E., Cubison, M. J., Esser-Gietl, J. K., Green, D. C., Gros, V., Heikkinen, L., Herrmann, H., Lunder, C., Minguillon, M. C., Mocnik, G., O'Dowd, C. D., Ovadnevaite, J., Petit, J. E., Petralia, E., Poulain, L., Priestman, M., Riffault, V., Ripoll, A., Sarda-Esteve, R., Slowik, J. G., Setyan, A., Wiedensohler, A., Baltensperger, U., Prevot, A. S. H., Jayne, J. T., and Favez, O.: ACTRIS ACSM intercomparison - Part 1: Reproducibility of concentration and fragment results from 13 individual Quadrupole Aerosol Chemical Speciation Monitors (Q-ACSM) and consistency with co-located instruments, Atmos. Meas. Tech., 8, 5063-5087, 10.5194/amt-8-5063-2015, 2015.

Cross, E. S., Slowik, J. G., Davidovits, P., Allan, J. D., Worsnop, D. R., Jayne, J. T., Lewis, D. K., Canagaratna, M., and Onasch, T. B.: Laboratory and ambient particle density determinations using light scattering in conjunction with aerosol mass spectrometry, Aerosol Sci. Technol., 41, 343-359, 10.1080/02786820701199736, 2007.

de Gouw, J. A., Middlebrook, A. M., Warneke, C., Goldan, P. D., Kuster, W. C., Roberts, J. M., Fehsenfeld, F. C., Worsnop, D. R., Canagaratna, M. R., Pszenny, A. A. P., Keene, W. C., Marchewka, M., Bertman, S. B., and Bates, T. S.: Budget of organic carbon in a polluted atmosphere: Results from the New England Air Quality Study in 2002, J. Geophys. Res.-Atmos., 110, 10.1029/2004jd005623, 2005.

DeCarlo, P. F., Slowik, J. G., Worsnop, D. R., Davidovits, P., and Jimenez, J. L.: Particle morphology and density characterization by combined mobility and aerodynamic diameter measurements. Part 1: Theory, Aerosol Sci. Technol., 38, 1185-1205, 10.1080/027868290903907, 2004.

Docherty, K. S., Jaoui, M., Corse, E., Jimenez, J. L., Offenberg, J. H., Lewandowski, M., and Kleindienst, T. E.: Collection Efficiency of the Aerosol Mass Spectrometer for Chamber-Generated Secondary Organic Aerosols, Aerosol Sci. Technol., 47, 294-309, 10.1080/02786826.2012.752572, 2013.



439 Drewnick, F., Schwab, J., Hogrefe, O., Peters, S., Husain, L., Diamond, D., Weber, R., and
440 Demerjian, K.: Intercomparison and evaluation of four semi-continuous PM2. 5 sulfate
441 instruments, Atmos. Environ., 37, 3335-3350, 2003.

442 Dzepina, K., Arey, J., Marr, L. C., Worsnop, D. R., Salcedo, D., Zhang, Q., Onasch, T. B., Molina,
443 L. T., Molina, M. J., and Jimenez, J. L.: Detection of particle-phase polycyclic aromatic
444 hydrocarbons in Mexico City using an aerosol mass spectrometer, Int. J. Mass spectrom., 263, 152-
445 170, 10.1016/j.ijms.2007.01.010, 2007.

446 Finlayson-Pitts, B. J., and Pitts, J. N.: Chemistry of the upper and lower atmosphere : theory,
447 experiments and applications, Academic Press, San Diego, Calif., xxii, 969 pp., 1999.

448 Hallquist, M., Wenger, J. C., Baltensperger, U., Rudich, Y., Simpson, D., Claeys, M., Dommen, J.,
449 Donahue, N. M., George, C., Goldstein, A. H., Hamilton, J. F., Herrmann, H., Hoffmann, T.,
450 Iinuma, Y., Jang, M., Jenkin, M. E., Jimenez, J. L., Kiendler-Scharr, A., Maenhaut, W., McFiggans,
451 G., Mentel, T. F., Monod, A., Prevot, A. S. H., Seinfeld, J. H., Surratt, J. D., Szmigielski, R., and
452 Wildt, J.: The formation, properties and impact of secondary organic aerosol: current and emerging
453 issues, Atmos. Chem. Phys., 9, 5155-5236, 2009a.

454 Hallquist, M., Wenger, J. C., Baltensperger, U., Rudich, Y., Simpson, D., Claeys, M., Dommen, J.,
455 Donahue, N. M., George, C., Goldstein, A. H., Hamilton, J. F., Herrmann, H., Hoffmann, T.,
456 Iinuma, Y., Jang, M., Jenkin, M. E., Jimenez, J. L., Kiendler-Scharr, A., Maenhaut, W., McFiggans,
457 G., Mentel, T. F., Monod, A., Prevot, A. S. H., Seinfeld, J. H., Surratt, J. D., Szmigielski, R., and
458 Wildt, J.: The formation, properties and impact of secondary organic aerosol: current and emerging
459 issues, Atmos. Chem. Phys., 9, 5155-5236, 2009b.

460 Hu, W., Campuzano-Jost, P., Day, D. A., Croteau, P., Canagaratna, M. R., Jayne, J. T., Worsnop,
461 D. R., and Jimenez, J. L.: Evaluation of the new capture vaporizer for aerosol mass spectrometers
462 (AMS) through field studies of inorganic species, Aerosol Sci. Technol., 51, 735-754,
463 10.1080/02786826.2017.1296104, 2017.

464 Huang, R.-J., Zhang, Y., Bozzetti, C., Ho, K.-F., Cao, J.-J., Han, Y., Daellenbach, K. R., Slowik,
465 J. G., Platt, S. M., Canonaco, F., Zotter, P., Wolf, R., Pieber, S. M., Bruns, E. A., Crippa, M.,
466 Ciarelli, G., Piazzalunga, A., Schwikowski, M., Abbaszade, G., Schnelle-Kreis, J., Zimmermann,
467 R., An, Z., Szidat, S., Baltensperger, U., Haddad, I. E., and Prevot, A. S. H.: High secondary aerosol
468 contribution to particulate pollution during haze events in China, Nature, 514, 218-222,
469 10.1038/nature13774

470 http://www.nature.com/nature/journal/v514/n7521/abs/nature13774.html - supplementary-
471 information, 2014.

472 IPCC: Climate Change 2014: Synthesis Report. Contribution of Working Groups I, II and III to the
473 Fifth Assessment Report of the Intergovernmental Panel on Climate Change, edited by: Pachauri,
474 R. K., and (eds.), L. A. M., IPCC, Geneva, Switzerland, 151 pp., 2014.



475 Jayne, J. T., Leard, D. C., Zhang, X. F., Davidovits, P., Smith, K. A., Kolb, C. E., and Worsnop,
476 D. R.: Development of an aerosol mass spectrometer for size and composition analysis of
477 submicron particles, Aerosol Sci. Technol., 33, 49-70, 10.1080/027868200410840, 2000.

478 Jimenez, J. L., Jayne, J. T., Shi, Q., Kolb, C. E., Worsnop, D. R., Yourshaw, I., Seinfeld, J. H.,
479 Flagan, R. C., Zhang, X. F., Smith, K. A., Morris, J. W., and Davidovits, P.: Ambient aerosol
480 sampling using the Aerodyne Aerosol Mass Spectrometer, J. Geophys. Res.-Atmos., 108,
481 10.1029/2001jd001213, 2003.

482 Jimenez, J. L., Canagaratna, M. R., Drewnick, F., Allan, J. D., Alfarra, M. R., Middlebrook, A. M.,
483 Slowik, J. G., Zhang, Q., Coe, H., Jayne, J. T., and Worsnop, D. R.: Comment on "The effects of
484 molecular weight and thermal decomposition on the sensitivity of a thermal desorption aerosol
485 mass spectrometer", Aerosol Sci. Technol., 50, I-XV, 10.1080/02786826.2016.1205728, 2016.

486 Kanakidou, M., Seinfeld, J. H., Pandis, S. N., Barnes, I., Dentener, F. J., Facchini, M. C., Van
487 Dingenen, R., Ervens, B., Nenes, A., Nielsen, C. J., Swietlicki, E., Putaud, J. P., Balkanski, Y.,
488 Fuzzi, S., Horth, J., Moortgat, G. K., Winterhalter, R., Myhre, C. E. L., Tsigaridis, K., Vignati, E.,
489 Stephanou, E. G., and Wilson, J.: Organic aerosol and global climate modelling: a review, Atmos.
490 Chem. Phys., 5, 1053-1123, 2005.

491 Kiendler-Scharr, A., Zhang, Q., Hohaus, T., Kleist, E., Mensah, A., Mentel, T. F., Spindler, C.,
492 Uerlings, R., Tillmann, R., and Wildt, J.: Aerosol Mass Spectrometric Features of Biogenic SOA:
493 Observations from a Plant Chamber and in Rural Atmospheric Environments, Environ. Sci.
494 Technol., 43, 8166-8172, 10.1021/es901420b, 2009.

495 Kondo, Y., Miyazaki, Y., Takegawa, N., Miyakawa, T., Weber, R. J., Jimenez, J. L., Zhang, Q.,
496 and Worsnop, D. R.: Oxygenated and water-soluble organic aerosols in Tokyo, J. Geophys. Res.-
497 Atmos., 112, 10.1029/2006jd007056, 2007.

498 Koop, T., Bookhold, J., Shiraiwa, M., and Pöschl, U.: Glass transition and phase state of organic
499 compounds: dependency on molecular properties and implications for secondary organic aerosols
500 in the atmosphere, Physical Chemistry Chemical Physics, 13, 19238-19255, 2011.

501 Liu, P., Ziemann, P. J., Kittelson, D. B., and McMurry, P. H.: Generating particle beams of
502 controlled dimensions and divergence .1. Theory of particle motion in aerodynamic lenses and
503 nozzle expansions, Aerosol Sci. Technol., 22, 293-313, 10.1080/02786829408959748, 1995a.

504 Liu, P., Ziemann, P. J., Kittelson, D. B., and McMurry, P. H.: Generating particle beams of
505 controlled dimensions and divergence .2. Experimental evaluation of particle motion in
506 aerodynamic lenses and nozzle expansions, Aerosol Sci. Technol., 22, 314-324,
507 10.1080/02786829408959749, 1995b.



508 Matthew, B. M., Middlebrook, A. M., and Onasch, T. B.: Collection efficiencies in an Aerodyne
509 Aerosol Mass Spectrometer as a function of particle phase for laboratory generated aerosols,
510 Aerosol Sci. Technol., 42, 884-898, 10.1080/02786820802356797, 2008.

511 McMurry, P. H., Wang, X., Park, K., and Ehara, K.: The relationship between mass and mobility
512 for atmospheric particles: A new technique for measuring particle density, Aerosol Sci. Technol.,
513 36, 227-238, 10.1080/027868202753504083, 2002.

514 Murphy, D. M.: The effects of molecular weight and thermal decomposition on the sensitivity of a
515 thermal desorption aerosol mass spectrometer, Aerosol Sci. Technol., 50, 118-125,
516 10.1080/02786826.2015.1136403, 2016.

517 Ng, N. L., Herndon, S. C., Trimborn, A., Canagaratna, M. R., Croteau, P. L., Onasch, T. B., Sueper,
518 D., Worsnop, D. R., Zhang, Q., Sun, Y. L., and Jayne, J. T.: An Aerosol Chemical Speciation
519 Monitor (ACSM) for Routine Monitoring of the Composition and Mass Concentrations of Ambient
520 Aerosol, Aerosol Sci. Technol., 45, 780-794, 10.1080/02786826.2011.560211, 2011.

521 Orsini, D. A., Ma, Y. L., Sullivan, A., Sierau, B., Baumann, K., and Weber, R. J.: Refinements to
522 the particle-into-liquid sampler (PILS) for ground and airborne measurements of water soluble
523 aerosol composition, Atmos. Environ., 37, 1243-1259, 10.1016/s1352-2310(02)01015-4, 2003.

524 Petit, J. E., Favez, O., Sciare, J., Crenn, V., Sarda-Esteve, R., Bonnaire, N., Mocnik, G., Dupont, J.
525 C., Haeffelin, M., and Leoz-Garziandia, E.: Two years of near real-time chemical composition of
526 submicron aerosols in the region of Paris using an Aerosol Chemical Speciation Monitor (ACSM)
527 and a multi-wavelength Aethalometer, Atmos. Chem. Phys., 15, 2985-3005, 10.5194/acp-15-2985-
528 2015, 2015.

529 Poschl, U.: Atmospheric aerosols: Composition, transformation, climate and health effects,
530 Angewandte Chemie-International Edition, 44, 7520-7540, 10.1002/anie.200501122, 2005.

531 Poschl, U., and Shiraiwa, M.: Multiphase Chemistry at the Atmosphere-Biosphere Interface
532 Influencing Climate and Public Health in the Anthropocene, Chemical Reviews, 115, 4440-4475,
533 10.1021/cr500487s, 2015.

534 Salcedo, D., Onasch, T. B., Dzepina, K., Canagaratna, M. R., Zhang, Q., Huffman, J. A., DeCarlo,
535 P. F., Jayne, J. T., Mortimer, P., Worsnop, D. R., Kolb, C. E., Johnson, K. S., Zuberi, B., Marr, L.
536 C., Volkamer, R., Molina, L. T., Molina, M. J., Cardenas, B., Bernabe, R. M., Marquez, C.,
537 Gaffney, J. S., Marley, N. A., Laskin, A., Shutthanandan, V., Xie, Y., Brune, W., Lesher, R.,
538 Shirley, T., and Jimenez, J. L.: Characterization of ambient aerosols in Mexico City during the
539 MCMA-2003 campaign with Aerosol Mass Spectrometry: results from the CENICA Supersite,
540 Atmos. Chem. Phys., 6, 925-946, 2006.



541 Shilling, J. E., Chen, Q., King, S. M., Rosenoern, T., Kroll, J. H., Worsnop, D. R., DeCarlo, P. F.,
542 Aiken, A. C., Sueper, D., Jimenez, J. L., and Martin, S. T.: Loading-dependent elemental
543 composition of α-pinene SOA particles, Atmos. Chem. Phys., 9, 771-782, 10.5194/acp-9-771-
544 2009, 2009a.

545 Shilling, J. E., Chen, Q., King, S. M., Rosenoern, T., Kroll, J. H., Worsnop, D. R., DeCarlo, P. F.,
546 Aiken, A. C., Sueper, D., Jimenez, J. L., and Martin, S. T.: Loading-dependent elemental
547 composition of alpha-pinene SOA particles, Atmos. Chem. Phys., 9, 771-782, 2009b.

548 Shiraiwa, M., Ammann, M., Koop, T., and Pöschl, U.: Gas uptake and chemical aging of semisolid
549 organic aerosol particles, Proc. Natl. Acad. Sci. USA, 108, 11003-11008, 2011.

550 Slowik, J. G., Stainken, K., Davidovits, P., Williams, L. R., Jayne, J. T., Kolb, C. E., Worsnop, D.
551 R., Rudich, Y., DeCarlo, P. F., and Jimenez, J. L.: Particle morphology and density characterization
552 by combined mobility and aerodynamic diameter measurements. Part 2: Application to
553 combustion-generated soot aerosols as a function of fuel equivalence ratio, Aerosol Sci. Technol.,
554 38, 1206-1222, 10.1080/027868290903916, 2004.

555 Sorooshian, A., Brechtel, F. J., Ma, Y. L., Weber, R. J., Corless, A., Flagan, R. C., and Seinfeld, J.
556 H.: Modeling and characterization of a particle-into-liquid sampler (PILS), Aerosol Sci. Technol.,
557 40, 396-409, 10.1080/02786820600632282, 2006.

558 Takegawa, N., Miyazaki, Y., Kondo, Y., Komazaki, Y., Miyakawa, T., Jimenez, J. L., Jayne, J. T.,
559 Worsnop, D. R., Allan, J. D., and Weber, R. J.: Characterization of an Aerodyne Aerosol Mass
560 Spectrometer (AMS): Intercomparison with other aerosol instruments, Aerosol Sci. Technol., 39,
561 760-770, 10.1080/02786820500243404, 2005.

562 Vaden, T. D., Song, C., Zaveri, R. A., Imre, D., and Zelenyuk, A.: Morphology of mixed primary
563 and secondary organic particles and the adsorption of spectator organic gases during aerosol
564 formation, Proc. Natl. Acad. Sci. USA, 107, 6658-6663, 2010.

565 Venkatachari, P., Zhou, L., Hopke, P. K., Schwab, J. J., Demerjian, K. L., Weimer, S., Hogrefe,
566 O., Felton, D., and Rattigan, O.: An intercomparison of measurement methods for carbonaceous
567 aerosol in the ambient air in New York City, Aerosol Sci. Technol., 40, 788-795,
568 10.1080/02786820500380289, 2006.

569 Virtanen, A., Joutsensaari, J., Koop, T., Kannosto, J., Yli-Pirilä, P., Leskinen, J., Mäkelä, J. M.,
570 Holopainen, J. K., Pöschl, U., and Kulmala, M.: An amorphous solid state of biogenic secondary
571 organic aerosol particles, Nature, 467, 824, 2010.

572 Weber, R. J., Orsini, D., Daun, Y., Lee, Y. N., Klotz, P. J., and Brechtel, F.: A particle-into-liquid
573 collector for rapid measurement of aerosol bulk chemical composition, Aerosol Sci. Technol., 35,
574 718-727, 10.1080/02786820152546761, 2001.



575 Yao, L., Ma, Y., Wang, L., Zheng, J., Khalizov, A., Chen, M., Zhou, Y., Qi, L., and Cui, F.: Role
576 of stabilized Criegee Intermediate in secondary organic aerosol formation from the ozonolysis of
577 α-cedrene, Atmos. Environ., 94, 448-457, http://dx.doi.org/10.1016/j.atmosenv.2014.05.063, 2014.

578 Yuan, C., Ma, Y., Diao, Y. W., Yao, L., Zhou, Y. Y., Wang, X., and Zheng, J.: CCN activity of
579 secondary aerosols from terpene ozonolysis under atmospheric relevant conditions, J. Geophys.
580 Res.-Atmos., 122, 4654-4669, 10.1002/2016jd026039, 2017.

581 Zelenyuk, A., Imre, D., Han, J.-H., and Oatis, S.: Simultaneous measurements of individual
582 ambient particle size, composition, effective density, and hygroscopicity, Anal. Chem., 80, 1401-
583 1407, 10.1021/ac701723v, 2008.

584 Zhang, Q., Jimenez, J. L., Canagaratna, M. R., Allan, J. D., Coe, H., Ulbrich, I., Alfarra, M. R.,
585 Takami, A., Middlebrook, A. M., Sun, Y. L., Dzepina, K., Dunlea, E., Docherty, K., DeCarlo, P.
586 F., Salcedo, D., Onasch, T., Jayne, J. T., Miyoshi, T., Shimono, A., Hatakeyama, S., Takegawa, N.,
587 Kondo, Y., Schneider, J., Drewnick, F., Borrmann, S., Weimer, S., Demerjian, K., Williams, P.,
588 Bower, K., Bahreini, R., Cottrell, L., Griffin, R. J., Rautiainen, J., Sun, J. Y., Zhang, Y. M., and
589 Worsnop, D. R.: Ubiquity and dominance of oxygenated species in organic aerosols in
590 anthropogenically-influenced Northern Hemisphere midlatitudes, Geophys. Res. Letts., 34,
591 10.1029/2007gl029979, 2007.

592 Zhou, W., Jiang, J., Duan, L., and Hao, J.: Evolution of Submicrometer Organic Aerosols during a
593 Complete Residential Coal Combustion Process, Environ. Sci. Technol., 50, 7861-7869,
594 10.1021/acs.est.6b00075, 2016.

595

Atmos. Meas. Tech. Discuss., https://doi.org/10.5194/amt-2018-45
Manuscript under review for journal Atmos. Meas. Tech.
Discussion started: 23 March 2018


Atmospheric Measurement Techniques Discussions

**Table 1. Summary of Chamber Experiment Conditions.**

| Precursor | # | VOC (ppbv) | $O_3$/OH [1] (ppbv/μL) | PM (μg $m^{-3}$) [2] | ρ (g $cm^{-3}$) [3] | f44 (%) [4] | ACSM/SMPS [5] | $R^2$ |
|---|---|---|---|---|---|---|---|---|
| isoprene | 1 | 200 | 300 μL | 140 | 1.09 | 0.057 | 2.14 | 0.99 |
| | 2 | 100 | 150 μL | 15 | 1.13 | 0.081 | 1.81 | 0.91 |
| | 3 | 60 | 90 μL | 8 | 1.26 | 0.138 | 1.40 | 0.85 |
| | 4 | 80 | 120 μL | 10 | 1.22 | 0.129 | 1.45 | 0.81 |
| | 5 | 160 | 60 μL | 22 | 1.24 | 0.160 | 1.24 | 0.96 |
| | 6 | 200 | 60 μL | 39 | 1.28 | 0.159 | 1.42 | 0.96 |
| α-pinene | 1 | 20 | 80 ppbv | 40 | 1.20 | 0.125 | 1.22 | 0.97 |
| | 2 | 60 | 75 μL | 110 | 1.26 | 0.135 | 1.44 | 0.99 |
| | 3 | 10 | 80 ppbv | 10 | 1.29 | 0.146 | 1.31 | 0.95 |
| | 4 | 60 | 60 ppbv | 11 | 1.25 | 0.152 | 1.17 | 0.88 |
| toluene | 1 | 30 | 75 μL | 18 | 1.21 | 0.146 | 0.92 | 0.95 |
| | 2 | 60 | 150 μL | 40 | 1.35 | 0.190 | 0.79 | 0.94 |
| | 3 | 30 | 50 μL | 16 | 1.10 | 0.079 | 1.52 | 0.81 |
| | 4 | 60 | 75 μL | 11 | 1.26 | 0.129 | 1.42 | 0.99 |

**[1] The amount of OH is expressed as the amount of methyl nitrite (μL)**

**[2] The concentration of PM (particulate matter) is the average mass concentration of SMPS in relative stable state which have already been amended by the measured density.**

**[3] ρ is the average value of density after density reaches a relative steady state.**

**[4] f44 is the average fraction of signal of m/z 44 among the total organic signal after f44 reaches a relatively stable value.**

**[5] ACSM/SMPS is the slope of the fitting curve.**

Atmos. Meas. Tech. Discuss., https://doi.org/10.5194/amt-2018-45
Manuscript under review for journal Atmos. Meas. Tech.
Discussion started: 23 March 2018


Atmospheric Measurement Techniques Discussions

603 **Table 2. Summary of Smog Chamber Experiments for CE calibration of $(NH_4)_2SO_4$ when coating with SOA.**

| Precursor | # | VOC (ppbv) | $O_3$/OH [1] (ppbv/μL) | $(NH_4)_2SO_4$ [2] (μg $m^{-3}$) | $(NH_4)_2SO_4$ [3] (μg $m^{-3}$) | Org (μg $m^{-3}$) [4] | f44 | $CE_{SOA}$ [4] |
|---|---|---|---|---|---|---|---|---|
| α-pinene | 1 | 20 | 50 μL | 57.5 | 66.0 | 33.5 | 0.202 | 0.333 |
| | 2 | 20 | 80 ppbv | 50.3 | 56.19 | 20.1 | 0.193 | 0.324 |
| | 3 | 60 | 80 ppbv | 43.9 | 48.37 | 55.8 | 0.147 | 0.327 |
| | 4 | 60 | 50 μL | 40.3 | 134.24 | 303 | 0.127 | 0.966 |
| toluene | 1 | 80 | 150 μL | 51.2 | 81.35 | 79.7 | 0.209 | 0.461 |
| | 2 | 80 | 100 μL | 55.6 | 71.0 | 25.6 | 0.237 | 0.370 |
| | 3 | 100 | 50 μL | 59.0 | 70.1 | 15.2 | 0.262 | 0.345 |
| | 4 | 60 | 200 μL | 48.3 | 57.5 | 30.7 | 0.210 | 0.345 |
| | 5 | 80 | 200 μL | 53.2 | 84.8 | 106.4 | 0.190 | 0.462 |

604 **[1] The amount of OH is expressed in terms of the amount of methyl nitrite injected (μL).**

605 **[2] The average mass concentration of $(NH_4)_2SO_4$ seed aerosol measured by ACSM before SOA was generated.**

606 **[3] The average mass concentration of SOA coated $(NH_4)_2SO_4$ seed aerosol measured by ACSM after coated.**

607 **[4] The generated SOA mass concentration after it reaches relatively constant value.**

608 **[5] CE of SOA coated $(NH_4)_2SO_4$. CE for dry, pure $(NH_4)_2SO_4$ was 0.28 in every experiment.**



609 **Figure Captions:**

610 Figure 1. Schematic of the collapsible atmospheric-pressure fluoropolymer (Teflon) smog chamber
611 and the instrument setup.

612 Figure 2. (a) A typical banana-shaped plot of aerosols generated from ozonolysis of α-pinene; (b)
613 Time series of aerosol mass concentration measured by Q-ACSM and integrated from SMPS
614 measurements, and the corresponding f44 and effective density of SOA calculated from the Q-
615 ACSM and APM measurements, respectively; (c) The number size-distributions of aerosols at one
616 hour interval during the experiment.

617 Figure 3. The response factor determined from the chamber experiment by fitting the Q-ACSM
618 measured mass concentration to that deduced from SMPS-APM measurements. Only data points
619 in relative steady-state was used.

620 Figure 4. Triangle plots of (left) α-pinene, (middle) toluene, (right) isoprene experiments. The color
621 codes represent data points in a certain experiment. f44 and f43 represent more oxidized and more
622 reduced form of organic components, respectively.

623 Figure 5. The linear correlations between Q-ACSM RFs (a) and effective density (b) with
624 respective to f44 obtained from all experiments. The error bars were evaluated from different data
625 points in the stable state within one experiments.

626 Figure 6. Organic, sulfate mass concentrations and f44 measured by Q-ACSM. Arrow 1 indicates
627 when $(NH_4)_2SO_4$ seed particles were introduced; Arrow 2 indicates when VOC precursor were
628 injected.

629 Figure 7. CE of SOA coated $(NH_4)_2SO_4$ particles. The color scale represents the $Org/SO_4$ mass
630 ratio.

631 Figure 8. Overall view of SOA particle phase, effective density (ρ), response factor(RF), relative
632 ionization efficiency(RIE) and collection efficiency(CE) variation with increasing O/C ratio in the
633 process of SOA oxidation.

634

Atmos. Meas. Tech. Discuss., https://doi.org/10.5194/amt-2018-45
Manuscript under review for journal Atmos. Meas. Tech.
Discussion started: 23 March 2018


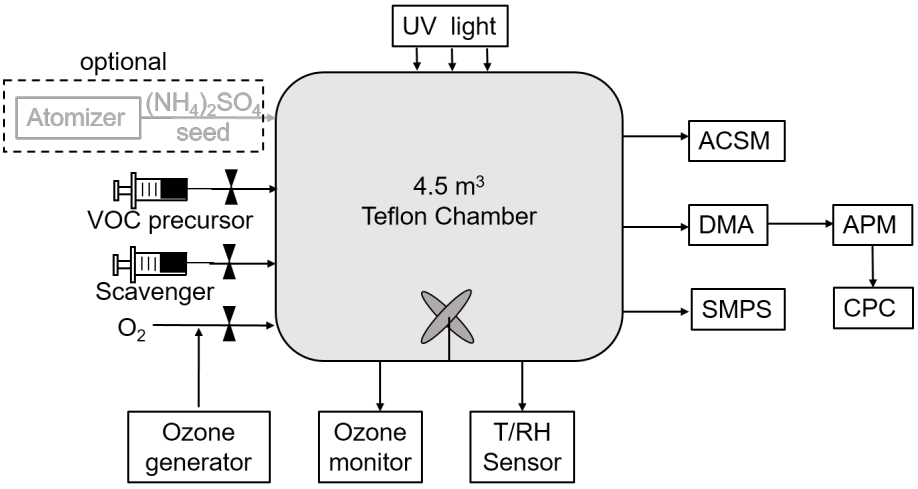


635

636 Figure 1. Schematic of the collapsible atmospheric-pressure fluoropolymer (Teflon) smog chamber

637 and the instrument setup.

638

Atmos. Meas. Tech. Discuss., https://doi.org/10.5194/amt-2018-45
Manuscript under review for journal Atmos. Meas. Tech.
Discussion started: 23 March 2018


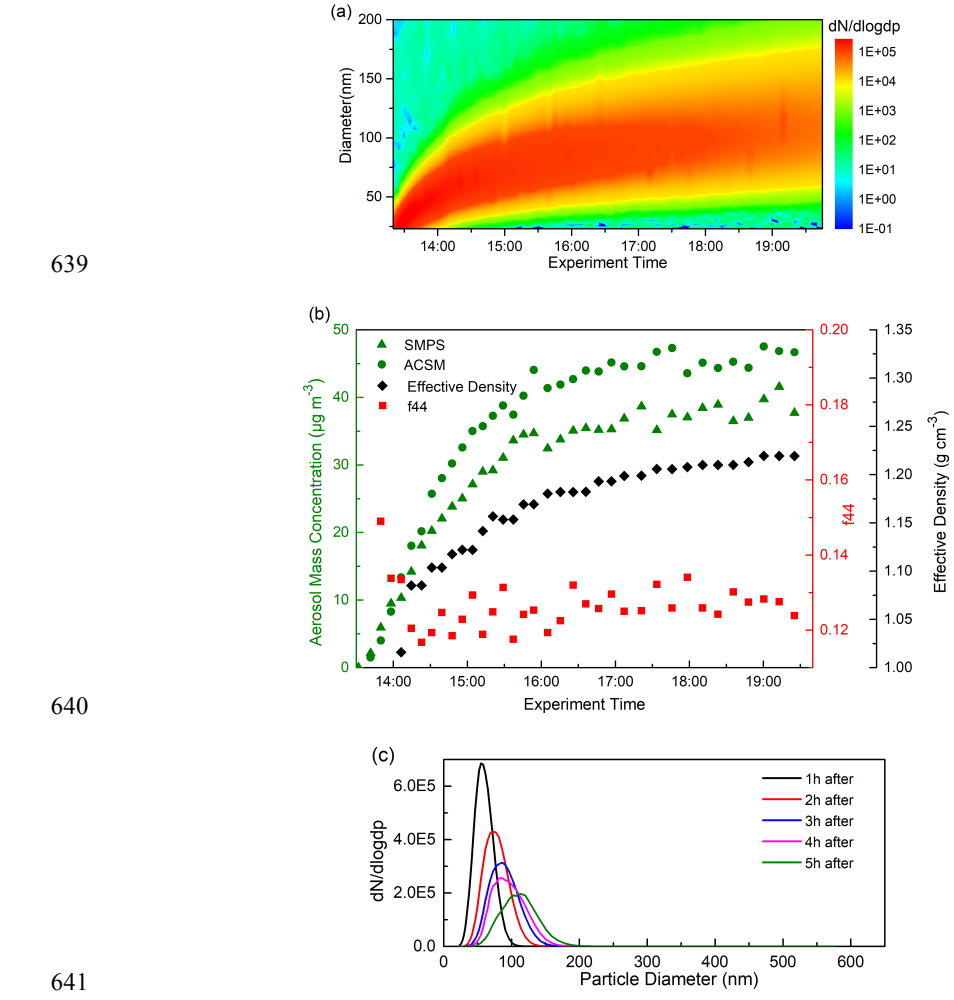


Figure 2. (a) A typical banana-shaped plot of aerosols generated from ozonolysis of α-pinene; (b) Time series of aerosol mass concentration measured by Q-ACSM and integrated from SMPS measurements, and the corresponding f44 and effective density of SOA calculated from the Q-ACSM and APM measurements, respectively; (c) The number size-distributions of aerosols at one hour interval during the experiment.

Atmos. Meas. Tech. Discuss., https://doi.org/10.5194/amt-2018-45
Manuscript under review for journal Atmos. Meas. Tech.
Discussion started: 23 March 2018


Atmospheric Measurement Techniques Discussions

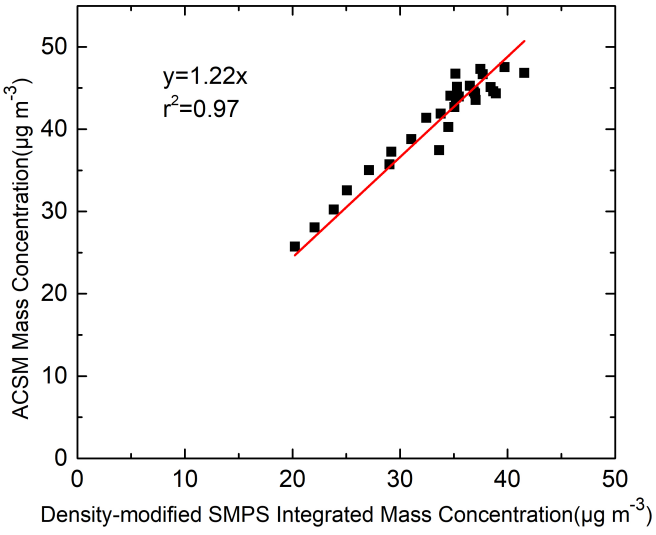


Figure 3. The response factor determined from the chamber experiment by fitting the Q-ACSM measured mass concentration to that deduced from SMPS-APM measurements. Only data points in relative steady-state was used.

Atmos. Meas. Tech. Discuss., https://doi.org/10.5194/amt-2018-45
Manuscript under review for journal Atmos. Meas. Tech.
Discussion started: 23 March 2018


Atmospheric Measurement Techniques Discussions

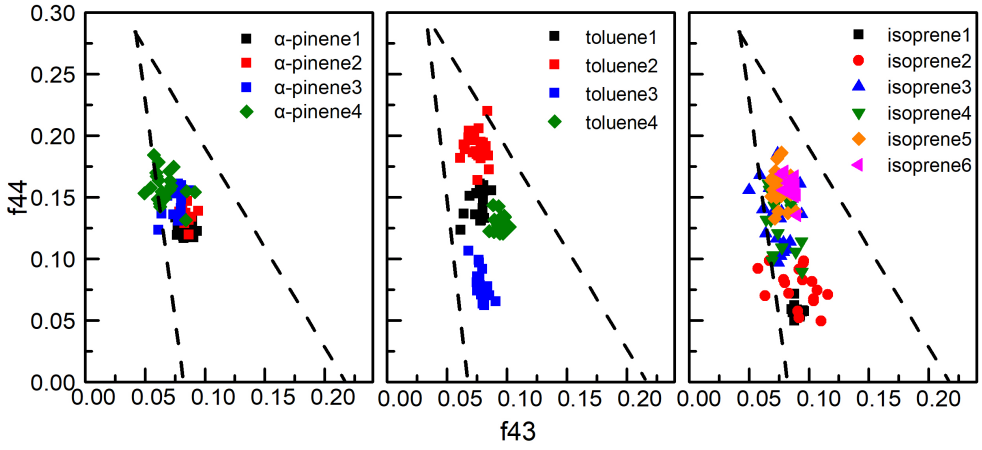


653

654 Figure 4. Triangle plots of (left) α-pinene, (middle) toluene, (right) isoprene experiments. The color

655 codes represent data points in a certain experiment. f44 and f43 represent more oxidized and more

656 reduced form of organic components, respectively.

657

Atmos. Meas. Tech. Discuss., https://doi.org/10.5194/amt-2018-45
Manuscript under review for journal Atmos. Meas. Tech.
Discussion started: 23 March 2018


Atmospheric Measurement Techniques Discussions

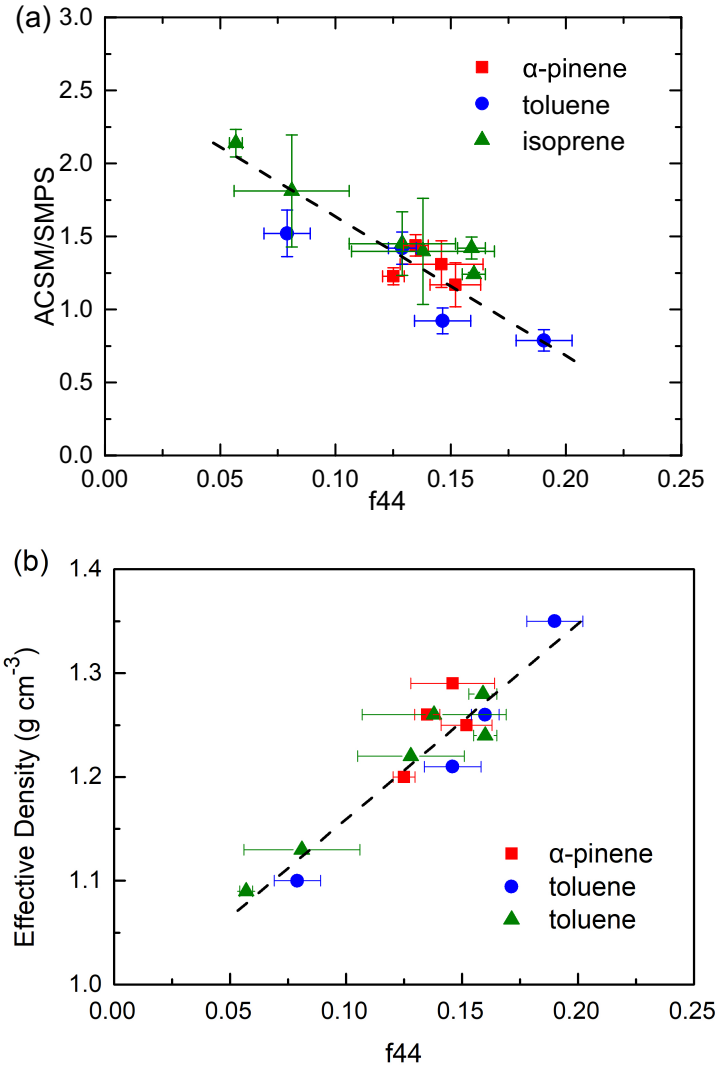


Figure 5. The linear correlations between Q-ACSM RFs (a) and effective density (b) with respective to f44 obtained from all experiments. The error bars were evaluated from different data points in the stable state within one experiments.

Atmos. Meas. Tech. Discuss., https://doi.org/10.5194/amt-2018-45
Manuscript under review for journal Atmos. Meas. Tech.
Discussion started: 23 March 2018


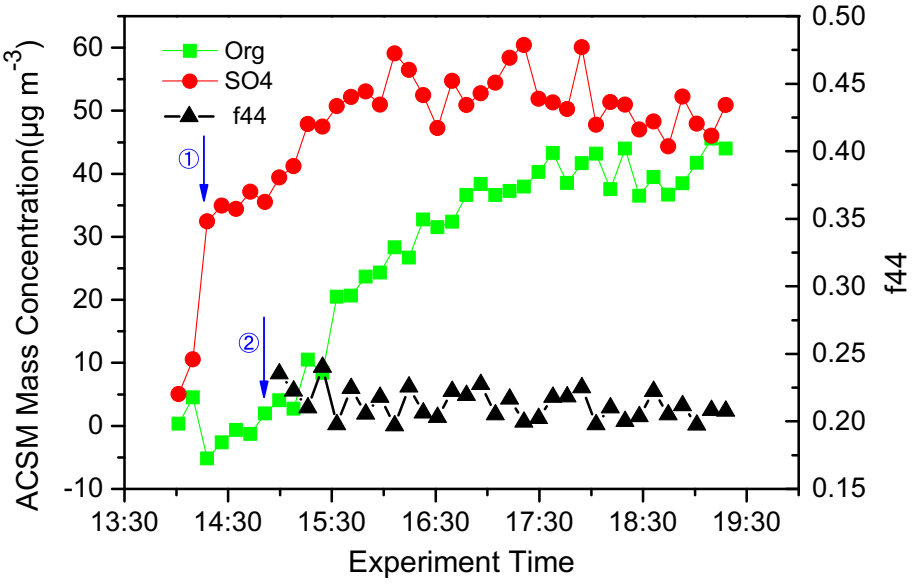


664

665 Figure 6. Organic, sulfate mass concentrations and f44 measured by Q-ACSM. Arrow 1 indicates
666 when $(NH_4)_2SO_4$ seed particles were introduced; Arrow 2 indicates when VOC precursor were
667 injected.

668

Atmos. Meas. Tech. Discuss., https://doi.org/10.5194/amt-2018-45
Manuscript under review for journal Atmos. Meas. Tech.
Discussion started: 23 March 2018


Atmospheric Measurement Techniques Discussions

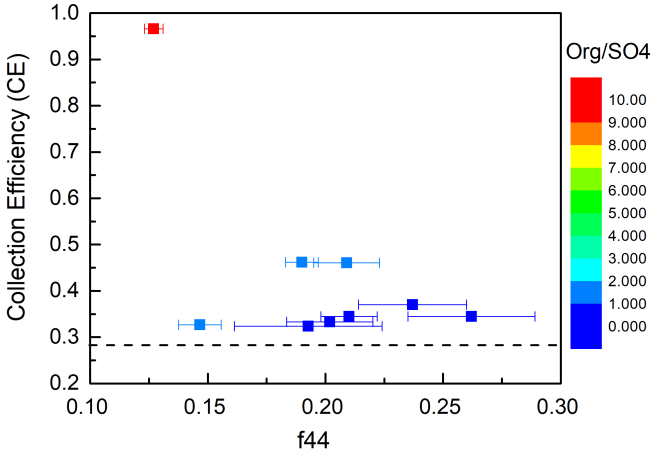


669

670 Figure 7. CE of SOA coated $(NH_4)_2SO_4$ particles. The color scale represents the $Org/SO_4$ mass

671 ratio.

672

Atmos. Meas. Tech. Discuss., https://doi.org/10.5194/amt-2018-45
Manuscript under review for journal Atmos. Meas. Tech.
Discussion started: 23 March 2018


Atmospheric Measurement Techniques Discussions

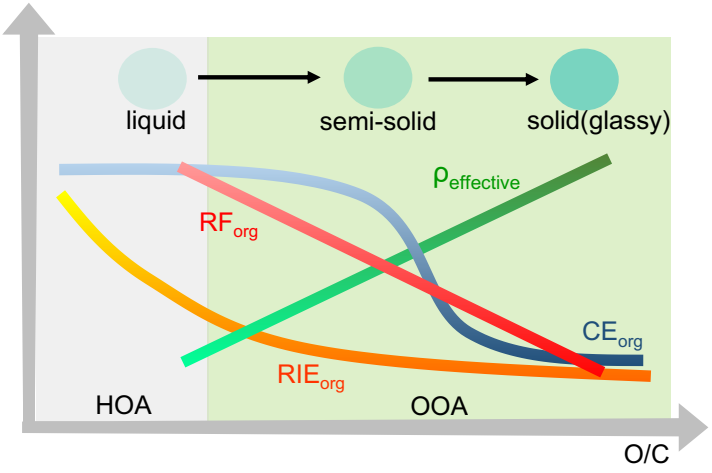


673

674 Figure 8. Overall view of SOA particle phase, effective density (ρ), response factor(RF), relative
675 ionization efficiency(RIE) and collection efficiency(CE) variation with increasing O/C ratio in the
676 process of SOA oxidation.